Desalination and Water Treatment
www.deswater.com

doi: 10.5004/dwt.2017.0425

60 (2017) 160–169
January

Preparation and characterization of activated carbon from Basra Ziziphus kernels and its adsorption characteristics for residual chlorine removal

Saad Abu-Alhail Al-Khalil

Department of Civil Engineering, College of Engineering, University of Basrah, 61004, Basra, Iraq, Mobile: +9647826480032; email: saadaboalheel@yahoo.com

Received 16 April 2016; Accepted 5 June 2016

ABSTRACT

Ziziphus kernels (ZKs) are used for production of activated carbon using a fluidized bed reactor. A chemical with phosphoric acid procedure is used to produce the required activated carbon. The ZKs are disposal material from a tree called Christ's thorn tree. ZKs are low in cost, and it be the may cause of solid waste pollution problems in Iraq. The adsorptive characteristics of Ziziphus kernels active carbons (ZKACs) were evaluated for their physical, chemical, surface and adsorption properties. Surface area is determined using Brunauer–Emmett–Teller (BET) surface area method. The microstructures of ZKACs were discovered using scanning electron microscopy (SEM) image technologies. The maximum iodine number of ZKACs is about 491 under the following conditions: impregnation ratio of 0.4, activation time of 1 h, activation temperature of 800°C, and particle size of 0.55 mm. The iodine number variation under all range of particle sizes is fluctuated between +12% and –11%. The obtained yield percent of ZKACs rises from 12 to 24.2 by raising the impregnation ratio range from 0.2 to 1.4 at 800°C and declines from 47 to 37 by raising the impregnation ratio range from 0.2 to 1.4 at 400°C. The highest removal of residual chlorine was obtained at height of 15 cm and with small grain size 1.5 mm of ZKACs.

Keywords: Ziziphus kernels; Active carbon; Adsorption; Chlorine removal

1. Introduction

Activated carbon is defined by its source and its properties, and it can be produced from almost any organic matter with high carbon content. Activated carbon is considered as one of the most important adsorbents. The carbonaceous material is the main part of its content which has microvoids in its surface and its structure. It is utilized industrially in the process of treatment for gas flue and volatile diluters [1]. Active carbon is the final product of activation process from different sources of carbonaceous materials with carbon contents ranged between 72% and 90%. The activation sequence usually starts with an initial raw material carbonization to get high carbon content in the samples [2]. It is utilized for purification, decolorization, and toxic organics and heavy metal ions removal in wastewater treatment [3]. It is used finally in advanced water treatment. Hereby, activated carbon's demand is growing. The type of raw material and activation factors determine the physical and chemical characteristics of activated carbon [4]. Activated carbon is classified into three types, such as powder, granular, and fibrous, and is considered as three shapes according to the sizes of activated carbon whereby each type has a specific application. Raw materials of activated carbon are selected according to some factors such as pureness, price, activation potential level, and availability. A number of agricultural products were utilized as raw material sources for activated carbon. These materials included coconut shells [5], wood [6,7], almond shells [8,9], olive stones [10,11], pecan shells [12–14], nutshells [15, 16] and other agricultural byproducts [17,18] but no one used ZKs as raw material for activated carbon. Many researchers have been working on the

1944-3994/1944-3986 © 2017 Desalination Publications. All rights reserved.

specific surface area and adsorbent capacity based on the types of chemicals and activation factors, whereas these researchers utilized variety of raw materials like petroleum residue, coconut shell and fly ash as raw active carbon materials [19, 20]. Many activation agents have dehydration and oxidation characteristics like zinc chloride, phosphoric acid, sulfuric acid, potassium hydroxide and calcium chloride that have been utilized for chemical activation [21, 22]. Activation is always implemented simultaneously with carbonization during chemical activation process. The chemical activation process is very efficient process for activated carbon used in water and wastewater treatment. Wastewater utilities have used activated carbon to remove harmful chlorine residual before discharge to the environment. The adsorption mechanism of activated carbon provides a highly efficient way to remove chlorine, although reaction rates may vary with chlorine concentration, type of residual, carbon particle size, pH and absorbed organic matter [23]. Activated carbon is very effective in removing free chlorine from water [24], whereas the mechanism of removal employed by activated carbon for dechlorination is not the adsorption phenomena that occur for organic compound removal.

The aims of this study were to utilize ZKs as raw materials for activated carbon production through chemical activation by phosphoric acid and evaluate its adsorption capacity for residual chlorine removal. In this study, the activation temperature, activation time, impregnation ratio and particle size investigated corresponding to iodine number and yield percent. Also, the change in the microstructure of the ZKs and produced activated carbon Ziziphus kernels active carbons (ZKACs) examined through scanning electron microscopy (SEM). The efficiency of ZKACs was investigated for chlorine residual removal in a fixed bed column with respect to operating conditions of the column, such as residual chlorine inlet concentration, adsorbate flow rate, bed height and adsorbent particle size.

2. Material and methods

2.1. Source of raw materials

ZKs used in this study were collected from Abu Al-Khasib, south of Basra city in the south region of Iraq, which is located about 25 km south of Basra city. ZKs were collected from fallen pieces under the trees called Christ's thorn. It is collected in plastic bags and transported to the laboratory where further testing procedures were carried out.

2.2. Production process

The activation steps of activated carbon from ZKs included five steps as shown in Fig. 1.

2.2.1. Sample preparation

ZKs were received as isolated from Ziziphus. Decanting separates any floated particulates easily with vigorous agitation. The remaining hard kernels were used in the experiments after continued process of washing, agitation, and decantation. Then, the clean kernels are dried at 115°C for about 1 d. Then, hard kernels are crushed and sieved through sieve analysis to the desired size. The resultant sieve cut is soaked in 97% C_2H_5OH for about 1 d to remove any undesirable materials; after that, the collected fractions were utilized to study the effect of the different parameters.

2.2.2. Activation agent

Specified size of 100 g ZKAC particles is mixed and shaken with 300 ml activation agent phosphoric acid of 86%. Using impregnation ratio of 0.2–1.4, the solution is left for 1 d at room temperature [25]. Then, the particles are rinsed by pure water and dried after filtration at 90°C for 1 d.

2.2.3. Activation

ZKs are dried at 110°C for 1 day. The particle with size 1–2 mm is put in a reactor furnace as shown in Fig. 2 and heated at a rate of 600°C/h from room temperature about 600°C and remained at this temperature for 90 min. The produced char is mixed with phosphoric acid where the ratio of char/H_2O/H_3PO_4 equal to 1/2.5/3.5 by weight, with constant speed mechanical stirring for 240 min and a temperature of 90°C. The impregnated char is dried all night at 115°C. The furnace reactor had the dry mixture under nitrogen gas flow of 0.144 m^3/h and heated at a rate of 600°C/h to a final temperature of 695°C, which remained for 120 min.

2.2.4. Leaching

To get activated carbon with excellent specific surface area, the materials of activated carbon under activation

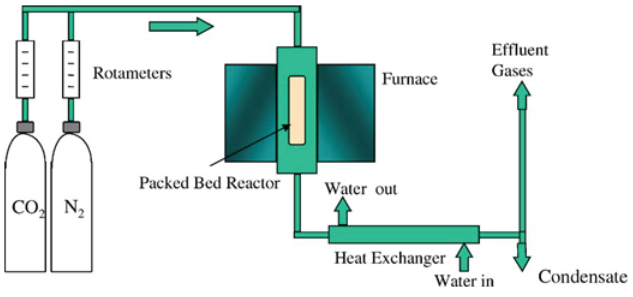

Fig. 2. Process diagram of Furnace Reactor.

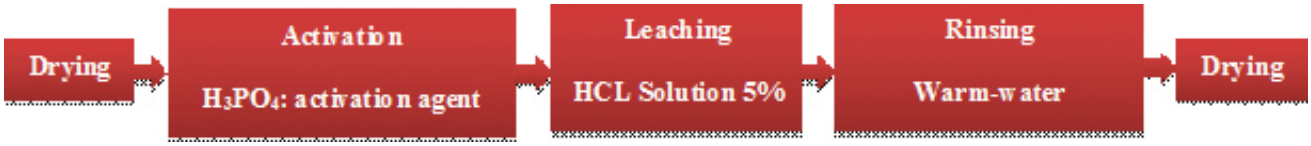

Fig. 1. Flow diagram of activation process.

process need to be washed with hydrochloric acid and rinsed with hot water for removing surfaces inorganic matter; therefore, all activated samples are washed with distilled water, transferred into 0.1 mol/L hydrochloric acid and agitated for 60 min to remove the remained acidity.

2.2.5. Rinsing and drying

All activated samples are rinsed with warm pure water. This rinsing is continued until pH of filtrating solution is neutral. Then, the produced ZKAC is dried at 105°C all night.

2.3. Experimental set up for adsorption of residual chlorine

Adsorption process was carried out by packed bed adsorption with height of 80 cm and diameter of 7 cm. Several experiments were implemented by changing the characteristics of granular activated carbons (GAC). Operating parameters for adsorption of residual chlorine are shown in Table 1.

3. Results and discussion

3.1. Characterization of produced active carbon

The composition structure of ZKAC is shown in Table 2. ZKACs are composed of a compact cellular structure with low porosity. At high temperature, phosphoric acid is mixed with ZKs; acid catalyst is appeared to promote reactions of bond cleavage and crosslinks formation by condensation and cyclization and also to chain with other organic species to build bridges of $PO_4^{=}$ that are considered as crosslink fragments of biological polymer [26]. There are various functions of acidic surface established in the oxidation surface in addition to the connection of different surface groups of oxygen and phosphorus which are establishing the porosity [27]. The cellulose dehydration via H_3PO_4 is same as alcohols dehydration under high temperatures. The oxides phosphorus can establish Carbon-Oxygen-Phosphorus bonds, whereas the oxides phosphorus works as Lewis acids. But, when the temperature is more than 900°C, the carbonaceous surface is empty from species of phosphorus bearing [28].

On the other hand, the characterization of the ZKACs could be done from identifying surface area, iodine number, yield, and so on.

Table 1
Experimental operating parameters for residual chlorine adsorption

Parameter	Range	Units
Initial chlorine concentration	2–3	ppm
Feed flow rate	500–1,300	cm^3/min
Height of bed	5–30	cm
Grain diameter of GAC	1.5–2.36	mm
Porosity of GAC	0.51–0.44	—

Table 2
Some properties of the Ziziphus kernels

Parameter	Value
Specific surface area (m^2/g)	911.22
Porous volume (cm^3/g)	0.729
Carbon (%)	64.154
Oxygen (%)	8.995
Phosphorus (%)	9.733

3.1.1. Surface area

The Brunauer–Emmett–Teller (BET) surface area method is based on a 1938 paper by Brunauer, Emmett, and Teller to measure the internal surface area of activated carbon. The mathematical model uses the nitrogen adsorption isotherm at low temperature and single layer adsorption. The DESOTEC R&D laboratory is equipped with a BET measuring instrument that, in addition to the internal surface area, also calculates the average pore size, pore volume and pore size distribution. Depending on the application, DESOTEC can offer activated carbon types ranging from 400 to more than 1500 m^2/g. Some properties of the ZKACs are presented in Table 2. The ZK is composed of carbon, but there is also oxygen from number of oxygenated surfaces. It is observed that phosphorus is presented due to treatment with phosphoric acid as an activation agent during the activation step. The ZKACs have surface area of 911.22 m^2/g and a porous volume of 0.729 cm^3/g.

3.1.2. Yield and the iodine number

Yield percent and iodine number are used to characterize the efficiency and quality of ZKAC. These characteristics of produced ZKACs are investigated through a number of influenced variables to find the conditions at which maximum yield and iodine number can be achieved. These variables include activation time, activation temperature, impregnation ratio and particle size of the produced ZKACs.

3.1.2.1. Yield of the activated carbon

The yield percent represents the mass ratio of produced ZKACs to ZKs. Yield investigation is related to four parameters which are time of activation, temperature of activation, impregnation ratio, and particle size.

$$\text{Yield } \% = \frac{\text{Mass of ZKAC}}{\text{Mass of ZKs (raw material)}} \quad (1)$$

The percentage yield of activated carbon is calculated as follows:

$$\text{Yield } \% = \frac{W_1}{(W_2 - W_3)} \quad (2)$$

where W_1 is the weight of end product, W_2 is the weight of impregnated powder and W_3 is the weight of reagent impregnated.

It is observed from Fig. 3 that yield percent declined from 21% to about 8.6% when the time of activation increased from 0.25 to 1 h while activation temperature, impregnation ratio and particle size are retained constantly. During the first half an hour, yield percent declined to about 9.2%. This happened

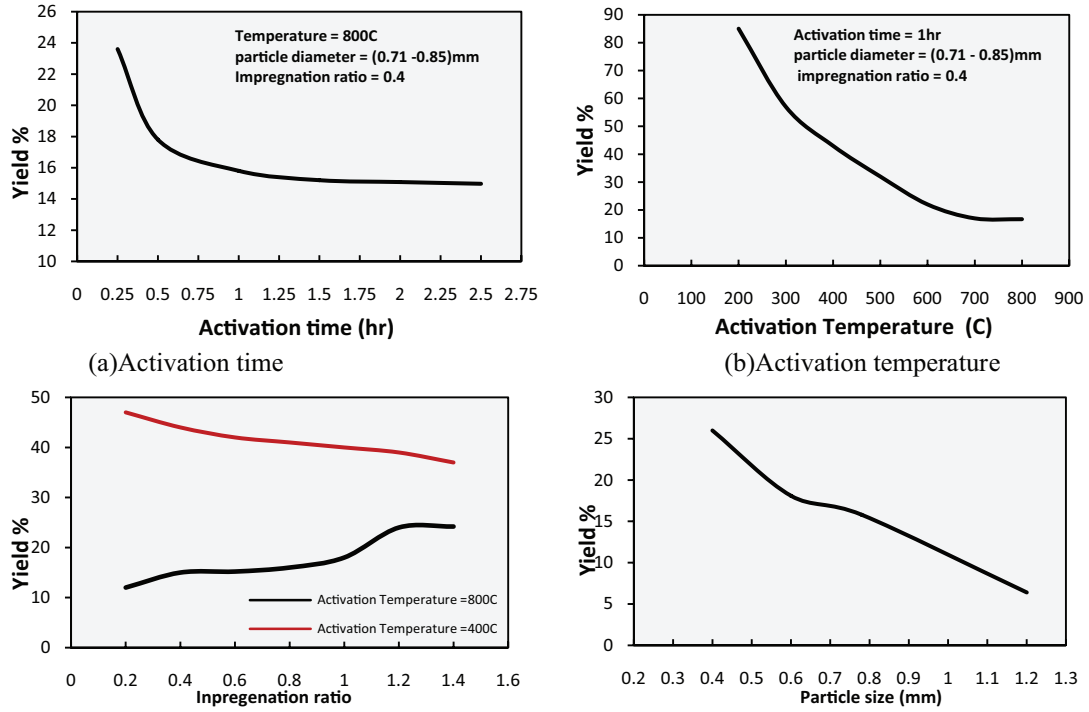

(a)Activation time

(b)Activation temperature

(c) impregenation ratio at activation time of 60 min ,and particle diameter from 0.71 to 0.85mm

(d) particel size at activation time of 60 min ,temperature of 800C˚,and impregenation ratio of 0.4.

Fig. 3. Effect of activation time, activation temperature, impregnation ratio, and particle size of yield percent: (a) activation time, (b) activation temperature, (c) impregnation ratio at activation time of 60 min, and particle diameter from 0.71 to 0.85 mm, (d) particle size at activation time of 60 min, temperature of 800°C, and impregnation ratio of 0.4.

due to rapid growth of volatile compounds to form stable compounds so the decline yield percent is proportional to the activation rate. Phosphoric acid works as an inhibitor of carbon oxidation at short contact time period less than half an hour, while the phosphorus bearing species leave the carbonaceous surface at long contact time period more than 0.5 h and less than 1 h, and activated carbon degradation comes to be simple. For that reason, the yield percent declines. After 1 h, activated carbon is built stable, and the yield percent becomes almost constant.

3.1.2.2. Iodine number

The amount of iodine absorbed (in milligrams) by 1 g of carbon when the iodine concentration of the residual filtrate is 0.02 N is called the iodine number; therefore, it is useful to characterize ZKACs by its iodine adsorptive capacity. The iodine adsorption was determined using the sodium thiosulfate ($Na_2S_2O_3$) volumetric method (ASTM D4607-86, 1999) [29]. The effect of activation time, temperature, impregnation ratio and particle size of iodine number is shown in Fig. 4.

The determination procedure of iodine number is listed as follows:

1. A weighed dry sample of the activated carbon is placed in a 250 mL dry Erlenmeyer flask and is fully wetted with 10 mL HCl 5%. The mixture is boiled for 30 s, and then cooled.
2. 100 mL of standardized iodine solution of normality (N) were poured into the Erlenmeyer flask, and the mixture is vigorously shaken for 30 s, then quick filtered through Whatman No. 2 V filter paper.
3. A volume of 50 mL of the filtrate solutions are titrated with standardized $Na_2S_2O_3$ (0.1 N) until the solution became pale yellow.
4. 2 mL of starch indicator solution (1,000 ppm) is added to solution where $Na_2S_2O_3$ titration continued until color of solution is removed and become watery color. The concentration of iodine adsorbed in the solution is calculated from the total titration volume of $Na_2S_2O_3$.

$$\text{Amount of iodine adsorbed} = \frac{500N_1 - 110N_2 \times V}{50}\text{g mol} \quad (3)$$

5. The iodine number of the activated carbon is then calculated by using the following equation:

$$\text{Iodine number} = \frac{W_I}{W_{AC}} * F \quad (4)$$

where F is the correction factor obtained after the calculation of the residual filtrate normality, WAC is the weight of activated carbon in grams, and W_I is the weight of adsorbed iodine in milligrams and is given by Eq. (5):

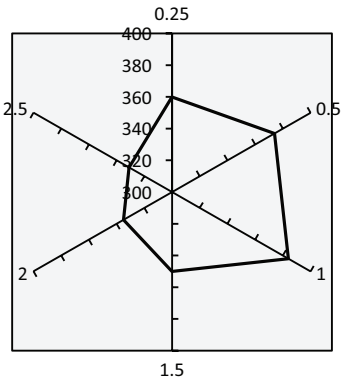

(a) Iodine number verses activation time

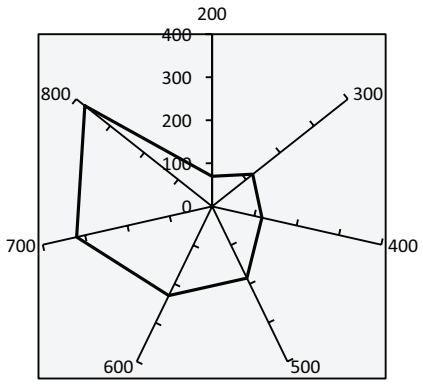

(b) Iodine number verses activation temperature

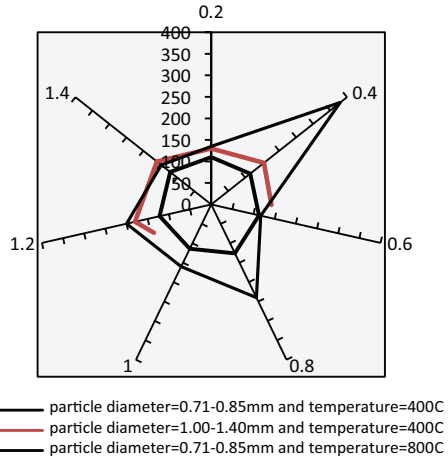

(c) Iodine number verses impregenation ratio at activation time of 60 min ,and particle diameter from 0.71 to 0.85mm

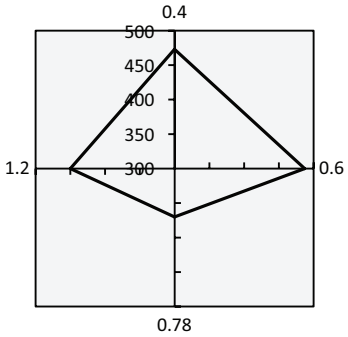

(d) Iodine number verses particel size at activation time of 60 min ,temperature of 800C,and impregenation ratio of 0.4.

Fig. 4. Effect of activation time, activation temperature, impregnation ratio, and particle size on iodine number: (a) iodine number vs. activation time, (b) iodine number vs. activation temperature, (c) Iodine number vs. impregnation ratio at activation time of 60 min, and particle diameter from 0.71 to 0.85 mm, (d) Iodine number vs. particle size at activation time of 60 min, temperature of 800°C, and impregnation ratio of 0.4.

$$W_I = 126.93 \times \left(\frac{100N_1 - 110N_2 \times V}{50} \right) \quad (5)$$

where N_1 is the normality of iodine solution, N_2 is the normality of $Na_2S_2O_3$ solution, and V is the volume of $Na_2S_2O_3$ solution used for titration.

3.1.3. Chemical structure

Fourier transform infrared (FTIR) transmission spectra were obtained to characterize the surface groups and structure [30, 31]. It can be used on the ZKs and the active carbons prepared from ZKs. Table 3 shows the FTIR spectra of the ZKs and ZKs-based active carbon. The ZKs contained many more bands than the prepared active carbons. The FTIR spectra of the ZKAC prepared at 700°C is shown in Fig. 5. It observed by other, the oxygen functional groups are increased by alkaline treatment especially phenolic groups [32]. In addition to that, carbon skeleton vibrations are noticed which are characteristic in ZKAC.

3.1.4. Thermogravimetric analysis

Thermogravimetric (TG) analysis—TG-DTG graphs are shown in Figs. 6 and 7—of the ZKAC was performed at N_2 rate of 6 L/h and a heating flux of 600°C/h up to 600°C. ZK exists little mass loss about 7% because of moisture at low temperatures up to 120°C as shown in Fig. 7. The mass stays approximately unchanged up to 230°C, but it is obviously decreased by losing 65% at temperature between 250 and 390°C because of volatile matter releasing due to precursor, cellulose, and hemicelluloses consumption [37, 38]. 22% is remaining material from initial raw material at a temperature of 400°C. Only 16.7% is remaining material from initial raw material at

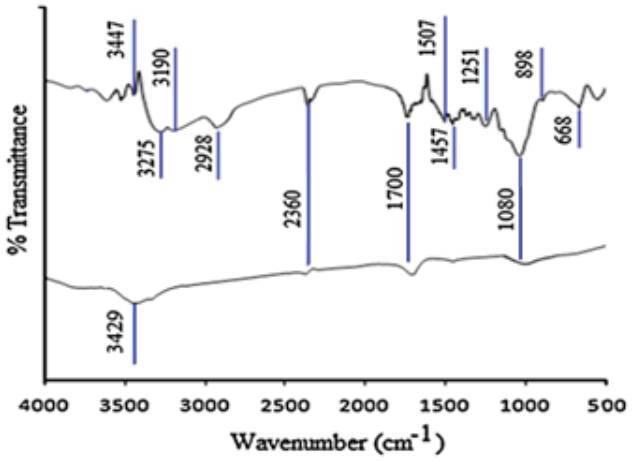

Fig. 5. FTIR spectra of ZKs and its active carbon.

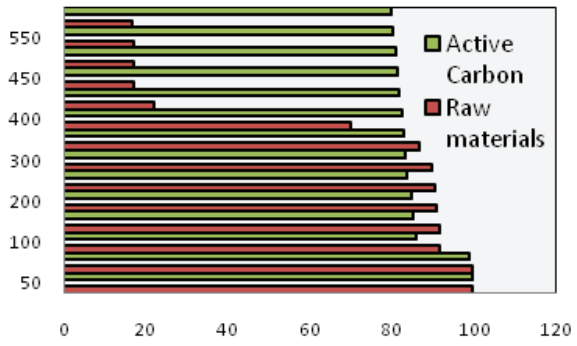

Fig. 6. TG thermogram of ZKs and its active carbon.

a temperature 600°C, which represents lignin decomposition as a structure with higher stability [39]. Furthermore, thermogram of ZKAC revealed a final yield of 82% for heating flux up to 600°C, which specifies a high thermal resistance for ZKAC. Derivative thermogravimetric (DTG) thermogram of ZKAC is shown in Fig. 7, whereas the maximum detected between 70 and 110°C is due to elimination of moisture content.

3.1.5. SEM analysis

Direct characterization of the pores using the SEM was found to be a good technique to actually see the pores and get actual measurements that can then be used to analyze and optimize the production process. It can be understood

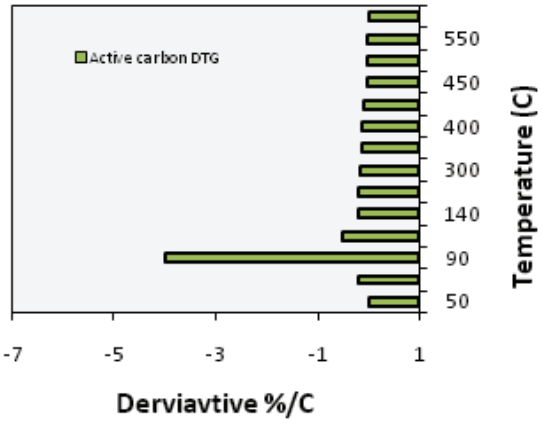

Fig. 7. DTG thermogram of ZKAC.

Table 3
Wave numbers of the principal bands in the FTIR spectra

Wave number (cm^{-1}) [33, 34]	Assignments [33, 34]	Ziziphus kernels active carbon	Ziziphus kernels
3,500–3,300	O-H intermolecular (H bonded)	3,429	3,447
2,930–2,900	C-H stretching vibration		2,928
2,720	C-H aldehydes		
1,734	C=O stretching in esters [35]		1,734
1,700	C=O of carboxylic groups	1,700	
1,625–1,610	C=O aromatic skeletal stretching		
1,580–1,570	C=C stretching band		
1,460–1,560	C=C aromatic rings, sym stretching of pyrone groups [34, 35]	1,490	1,507 and 1,457
1,450–1,420	C-H asym. bending		
1,375–1,317	C-H asym. and asym. bending		
1,284–1,240	C-O asym. stretching of aromatic ethers, esters, and phenols		1,251
1,260–1,000	C-O in carboxyl acids, alcohol, phenols, and esters or the P=O bond in phosphate esters	1,080	1,036
950–750	C-H out of plane bending to benzene derivative [36]		898
700–400	C-C stretching		

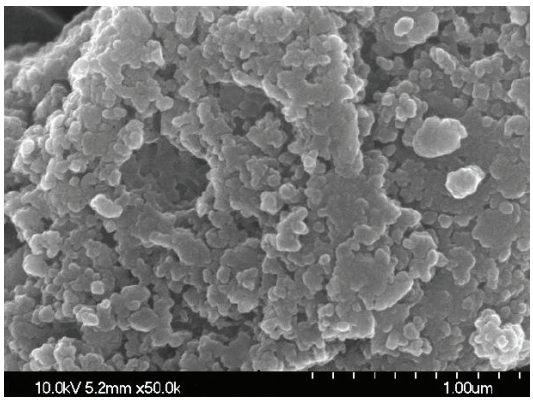

(a)

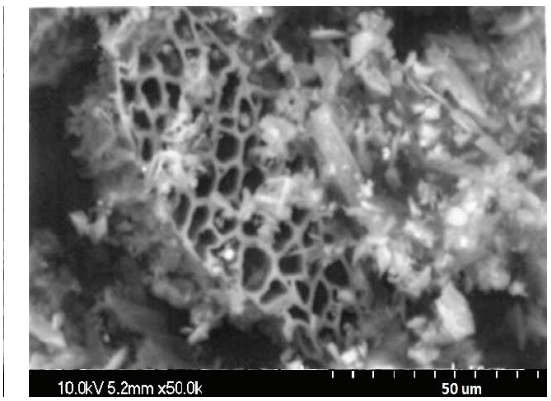

(b)

Fig. 8. SEM images of the Ziziphus kernels active carbon.

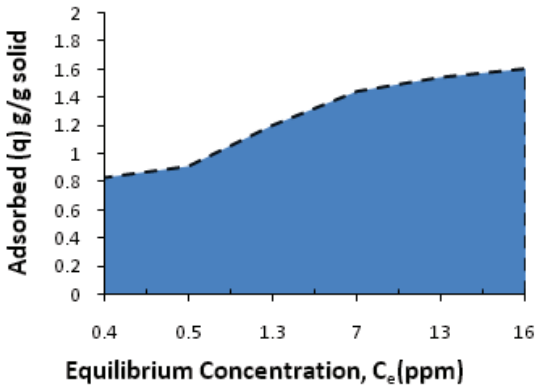

Fig. 9. Adsorption of residual chlorine using commercial GAC.

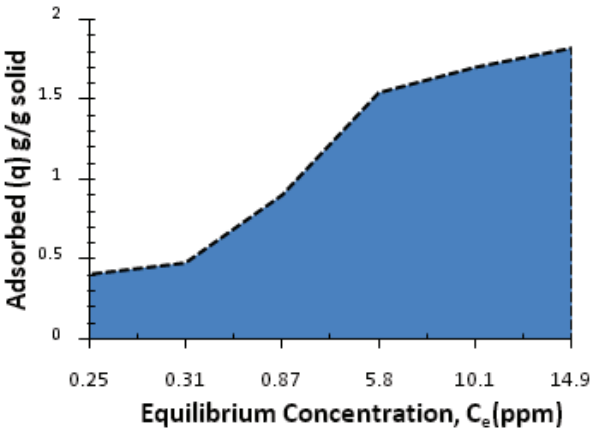

Fig. 10. Adsorption of residual chlorine on produced ZKACs.

from SEM image as shown in Fig. 8 that there are large, irregular voids on the external surfaces of ZKAC which point to the porosity of ZKAC formed by a violent interaction of reagent phosphoric acid during activation. During pyrolysis, pore enlargement in the ZKAC is essential as this would improve the pore volume and surface area too of the ZKAC by stimulating phosphoric acid diffusion molecule to the pores and in that way increasing the phosphoric acid carbon reaction, which would then form more pores in the ZKAC. Activation with phosphoric acid denotes phosphorus interaction between graphene layers and H_2 creation, which effects to minimize the quantity of surface O2 catalytically active [40].

3.2. Adsorption Mechanism of ZKACs

Batch experiments were performed to characterize the adsorption isotherms for both the produced ZKACs and the conventional GAC at 27°C. The equilibrium adsorption capacity of the produced ZKACs (Q) obtained in the present study was compared with conventional GAC for residual chlorine adsorption as shown in Figs. 9 and 10. The results showed that the produced ZKACs have a great potential as an adsorbent for residual chlorine in water systems and can compete favorably with conventional adsorbents.

3.3. Influence parameters on adsorption rate of chlorine

3.3.1. ZKAC height

The effect of ZKAC height on effluent chlorine concentration (C_e) is shown in Fig. 11. At an inlet chlorine concentration of 2,500 mg/l, flow rate of 5 L/min, and particle diameter of 2.9 mm. The ZKAC heights ranged from 5 to 15 cm. It is noticed that as the ZKAC height increases 5, 10, and 15 cm, respectively, the operation time of BP increases from 45 to 247 min. This shows that at a small ZKAC height, the effluent chlorine concentration ratio increases more rapidly than higher ZKAC height. Furthermore, a small ZKAC height corresponds to less amount of chlorine adsorbent. As a result, a small capacity of ZKAC height to adsorb chlorine from its solution and a faster increase in the flow of adsorption is expected.

3.3.2. Inlet concentration of residual chlorine

The effect of the initial chlorine concentration in the influent is one of the limitation factors and the main process parameter. Fig. 12 shows the effect of inlet residual chlorine concentration in the adsorption breakthrough. The chlorine concentrations ranged from 2,000 to 3,000 mg/l. During these simulations, other parameters are kept constant at

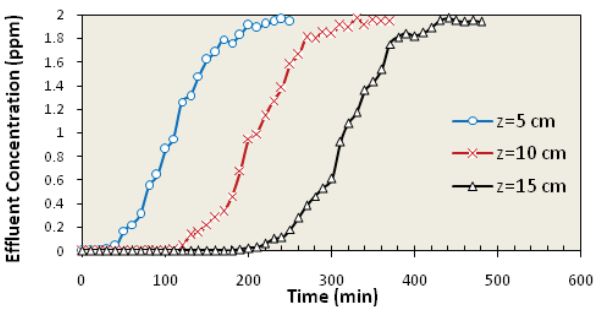

Fig. 11. Effect of ZKAC height on chlorine adsorption.

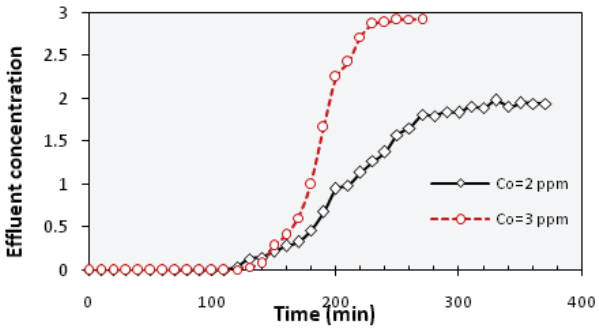

Fig. 12. Effect of inlet residual chlorine concentration on its adsorption

ZKAC height of 5 cm, water flow of 5 L/min, and ZKAC particle diameter of 2.9 mm. It is noticed that as the inlet chlorine concentration increases from 2,000 to 3,000 mg/l, the breakpoint time decreases from 160 to 144 min. For high feed concentration, steeper breakthrough curves are found, because of the low mass transfer flux from the bulk solution to the adsorbent surface due to the weaker driving force. In addition, at high concentration, the isotherm gradient is lower, yielding a higher driving force along the pores. Thus, the equilibrium is attained faster for values of high chlorine concentration.

3.3.3. Feed discharge

The results of various flow rates are plotted for a bed height of 5 cm, ZKACs diameter of 2.9mm, and an inlet chlorine concentration of 2,000 mg/l as shown in Fig. 13. This figure shows that the break time has been appeared earlier with high flow rate. On the other hand, the breakthrough curve was steeper with higher flow rate. This is because of the residence time of the solute in the column, which is not long enough for adsorption equilibrium to be reached at high flow rate; therefore, the residual chlorine solution leaves the column before equilibrium occurs. Furthermore, a fixed adsorption capacity of bed based on the same driving force gives rise to a shorter time of saturation at high flow rate.

3.3.4. Effect of particle size

In order to investigate the effect of ZKAC particle diameter on the adsorption dynamics, a sieve analysis was

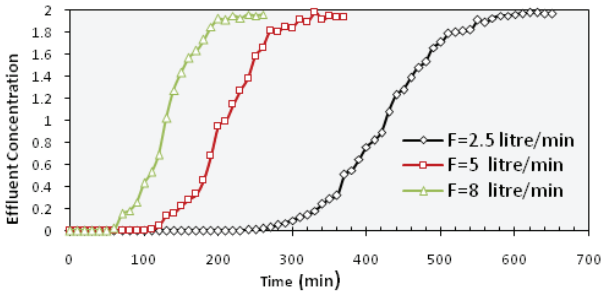

Fig. 13. Effect of feed discharge on chlorine adsorption.

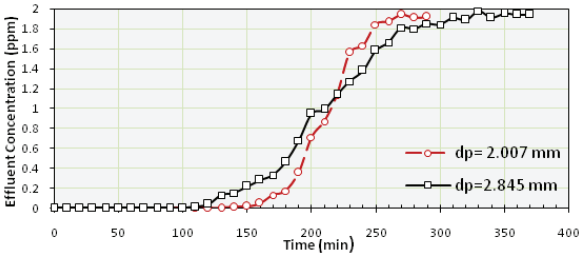

Fig. 14. Effect of particle size on chlorine adsorption.

conducted to separate the adsorbent particles to the sizes of interest; two with different average ZKAC particle diameter was selected to perform the investigations in the adsorption rig. The effect of particle size on the effluent concentration is shown in Fig. 14. During these experiments, other parameters such as flow rate, ZKAC height, and inlet chlorine concentration are kept constant at 2,500 mg/l influent concentration, 5 cm ZKAC height, and 5 L/min water flow rate. Fig. 14 revealed that as the ZKAC particle diameter increases from 2.007 to 2.845 mm, the steepness of the breakthrough curve decreases. The breakpoint time increased from 150 to 180 min. This can be explained as the diameter of the particle increases, the thickness of the stagnant film around the particles increases, and also the total length of the path inside the pores increases. Under these conditions, the overall kinetics of the process is slow, because the time for a molecule of chlorine to reach the adsorption site is more, as the diffusional path along the pores is large.

4. Conclusions

The ZKs are disposal material from tree called Christ's thorn. ZKs are low in cost, and it may cause solid waste pollution problems in Iraq; therefore, the wastes of ZKs were used as raw materials for the production of activated carbon using phosphoric acid as an activation agent. The major findings from this study can be described by the following points:

1. The major characteristics findings of ZKAC can be described as follows:
   (a) The increasing of particle size leads to decreasing in the yield percent. This is due to compact cellular structure and low porosity of ZKAC and high viscosity of phosphoric acid that causes low diffusion coefficient through the particles, whereas this can be considered as abnormal behavior for ZKAC.

(b) The obtained yield percent of ZKA Crises from 12 to 24.2 by raising the impregnation ratio range from 0.2 to 1.4 at 800°C and declines from 47 to 37 by raising the impregnation ratio range from 0.2 to 1.4 at 400°C.
(c) The iodine number rises extremely with activation temperature increasing, whereas a fluctuation in the iodine number value is observed by increasing impregnation ratio at same the temperature.
(d) The maximum iodine number of ZKACs is about 491 under the following conditions: impregnation ratio of 0.4, activation time of 1 h, activation temperature of 800°C and particle size of 0.55 mm. The iodine number variation under all range of particle sizes has fluctuated between +12% and –11%.
(e) The investigations of SEM analysis and FTI Spectroscopy on the surface of ZKAC have verified the occurrence of a porous structure and various functionalities.

2. Removal of residual chlorine
(a) Adsorption of residual chlorine is influenced by various parameters such as grains size, bed height, inlet residual chlorine concentration, discharge and ZKAC particle diameter.
(b) The prepared activated carbon from ZKs is an effective adsorbent for the removal of residual chlorine from aqueous solutions.
(c) The highest removal of residual chlorine was obtained at height of 15 cm and with small grain size 1.5 mm of ZKAC.

References

[1] B.S. Girgis, S.S. Yunis, A.M. Soliman, Characteristics of activated carbon from peanut hulls in relation to conditions of preparation, Mater. Lett., 57 (2002) 164–172.
[2] L. Daza, S. Mendioroz, J.A. Pajares, Preparation of Rh/active carbon catalysts by adsorption in organic media, Carbon 24 (1986) 33–41.
[3] PL Walker Jr. , Chemistry and Physics of Carbon ,volume one, Marcel Dekker Inc., New York (1965), ISBN 0-8247-0987, pp. 121–202.
[4] R. DiPanfilo, N.O. Egiebor, Activated carbon production from synthetic crude coke, Fuel Process. Technol., 46 (1996) 157–169.
[5] C.J. Kirubakaran, K. Krishnaiah, S.K. Seshadri, Experimental study of the production of activated carbon from coconut shells in a fluidized bed reactor. Ind. Eng. Chem. Res., 30 (1991) 2411–2416, doi: 10.1021/ie00059a008.
[6] H. Benaddi, J.N. Rouzaud, J. Conard, D. Legras, F. Beguin, Influence of the atmosphere in the chemical activation of wood by phosphoric acid, Carbon, 36 (1998) 306–309.
[7] M.J. Mazzetti, F. Derbyshire, Activated carbons from yellow poplar and white oak by H3PO4 activation, Carbon, 36 (1998) 1085–1097.
[8] F. Rodríguez-Reinoso, J. Garrido, J.M. Martín-Martínez, M. Molina-Sabio, R. Torregrosa, The combined use of different approaches in the characterization of microporous carbons, Carbon: Proceedings of the Conference on Porosity and Carbon materials: Measurements and applications 27 (1989) 23–32.
[9] C.A. Toles, W.E. Marshall, M.M. Johns, L.H. Wartelle, A. McAloon, Acid-activated carbons from almond shells: physical, chemical and adsorptive properties and estimated cost of production, Bioresour. Technol., 71 (2000) 87–92.
[10] T.T. Al-Khalid, N.M. Haimour, S.A. Sayed, B.A. Akash, Activation of olive-seed waste residue using CO2 in a fluidized-bed reactor, Fuel Process. Technol., 57 (1998) 55–64.
[11] A. Baçaoui, A. Yaacoubi, A. Dahbi, C. Bennouna, R. Phan Tan Luu, F.J. Maldonado-Hodar, J. Rivera-Utrilla, C. Moreno-Castilla, Optimization of conditions for the preparation of activated carbons from olive-waste cakes, Carbon, 39 (2001) 425–432.
[12] R.A. Shawabkeh, D.A. Rockstraw, R.K. Bhada, Copper and strontium adsorption by a novel carbon material manufactured from pecan shells, Carbon, 40 (2002) 781–786.
[13] R.R. Bansode, J.N. Losso, W.E. Marshall, R.M. Rao, R.J. Portier, Adsorption of volatile organic compounds by pecan shell- and almond shell-based granular activated carbons, Bioresour. Technol., 90 (2003) 175–184.
[14] S.A. Dastgheib, D.A. Rockstraw, A model for the adsorption of single metal ion solutes in aqueous solution onto activated carbon produced from pecan shells, Carbon, 40 (2002) 1843–1851.
[15] C.A. Toles, W.E. Marshall, M.M. Johns, Phosphoric acid activation of nutshells for metals and organic remediation: Process optimization, J. Chem. Technol. Biotechnol., 72 (1998) 255–263.
[16] M.A. Abdi, M. Mahdiarfar, A. Jalilian, A. Ahmadpour, A.R. Mirhabibi, Preparation of carbon molecular sieve from a new natural source, International Conference on Carbon, Lexington, United States 7 (2001) 14–19.
[17] W.T. Tsai, C.Y. Chang, S.Y. Wang, C.F. Chang, S.F. Chien, H.F. Sun, Utilization of agricultural waste corn COB for the preparation of carbon adsorbent, J. Environ. Sci. Health B., 36 (2001) 677–686.
[18] C.C. Wu, W.P. Walawender, L.T. Fan, Chemical agents for production of activated carbons from extrusion cooked grain products, Carbon: Proceedings 1997, 23rd Biennial Conference on Carbon, University Park 7 (1997) 18–23.
[19] A. Ahmadpour, D.D. Do, The preparation of active carbons from coal by chemical and physical activation, Carbon, 34 (1996) 471–479.
[20] A. Ahmadpour, D.D. Do, The preparation of activated carbon from macadamia nutshell by chemical activation, Carbon, 35 (1997) 1723–1732.
[21] M. Molina-Sabio, F. RodRíguez-Reinoso, F. Caturla, M.J. Sellés, Porosity in granular carbons activated with phosphoric acid, Carbon, 33 (1995) 1105–1113.
[22] J. Hayashi, A. Kazehaya, K. Muroyama, A.P. Watkinson, Preparation of activated carbon from lignin by chemical activation, Carbon, 38 (2000) 1873–1878.
[23] V.L. Snoeyink, M.T. Suidan, T. Makram, Dechlorination by activated carbon and other reducing agents, In: J.D. Johnson, Disinfection: water and wastewater. Ann Arbor, Ann Arbor Science (1975) 339–58.
[24] Robert Potwora "Chlorine and Chloramine Removal with Activated Carbon", Water Conditioning & Purification (WCP) JUNE 2009. http://www.wcponline.com/pdf/Potwora.pdf.
[25] F. Caturla, M. Molina-Sabio, F. Rodríguez-Reinoso, Preparation of activated carbon by chemical activation with ZnCl2, Carbon, 29 (1991) 999–1007.
[26] M. Jagtoyen, F. Derbyshire, Activated carbons from yellow poplar and white oak by H3PO4 activation, Carbon, 36 (1998) 1085–1097.
[27] S.A. Dastgheib, D.A. Rockstraw, Pecan shell activated carbon: synthesis, characterization, and application for the removal of copper from aqueous solution, Carbon, 39 (2001) 1849–1855.
[28] S. Labruquere, R. Pailler, X. Bourrat, R. Naslain, Enhancement of the oxidation resistance of carbon fibers in C/C composites via surface treatments, Key Eng. Mat., 132–136 (1997) 1938–1941.
[29] ASTM D4607-86, Standard test method for determination of iodine number of active carbon, Designation, (1999) 4607–1994.
[30] S. Sugashini, K. Mohamed Meera Sheriffa Begum, Adsorption and desorption studies on the performance of Fe-loaded chitosan carbonized rice husk for metal ion removal, Desal. Water Treat., 51 (2013) 7764–7774.
[31] K.A. Krishnan, S.S. Suresh, S. Arya, K.G. Sreejalekshmi, Adsorptive removal of 2,4-dinitrophenol using active carbon: kinetic and equilibrium modeling at solid–liquid interface, Desal. Water Treat., 54 (2015) 1850–1861.

[32] H-.L. Chiang, C.P. Huang, P.C. Chiang, The surface characteristics of activated carbon as affected by ozone and alkaline treatment, Chemosphere, 47 (2002) 257–265.
[33] A.H. El-Sheikh, A.P. Newman, H.K. Al-Daffaee, S. Phull, N. Cresswell, Characterization of activated carbon prepared from a single cultivar of Jordanian Olive stones by chemical and physicochemical techniques, J. Anal. Appl. Pyrol., 71 (2004) 151–164.
[34] J.C. Vaghetti, E.C. Lima, B. Royer, B.M. da Cunha, N.F. Cardoso, J.L. Brasil, S.L. Dias, Pecan nutshell as biosorbent to remove Cu(II), Mn(II) and Pb(II) from aqueous solutions, J. Haz. Mat., 162 (2009) 270–280.
[35] M.A. Montes-Morán, D. Suárez, J.A. Menéndez, E. Fuente, On the nature of basic sites on carbon surfaces: an overview, Carbon 42 (2004) 1219–1225.
[36] H. Demiral, İ. Demiral, B. Karabacakoğlu, F. Tümsek, Production of activated carbon from olive bagasse by physical activation, Chem. Eng. Res. Des., 89 (2011) 206–213.
[37] B. Cagnon, X. Py, A. Guillot, F. Stoeckli, G. Chambat, Contributions of hemicellulose, cellulose and lignin to the mass and the porous properties of chars and steam activated carbons from various lignocellulosic precursors, Bioresour. Technol., 100 (2009) 292–298.
[38] Ç. Şentorun-Shalaby, M.G. Uçak-Astarlıogˇlu, L. Artok, Ç. Sarıcı, Preparation and characterization of activated carbons by one-step steam pyrolysis/activation from apricot stones, Microporous Mesoporous Mater., 88 (2006) 126–134.
[39] B.S. Girgis, A-.N.A. El-Hendawy, Porosity development in activated carbons obtained from date pits under chemical activation with phosphoric acid, Microporous Mesoporous Mater., 52 (2002) 105–117.
[40] M.A. Lillo-Ródenas, J.P. Marco-Lozar, D. Cazorla-Amorós, A. LinaresSolano, Activated carbons prepared by pyrolysis of mixtures of carbon precursor/alkaline hydroxide, J. Anal. Appl. Pyrol., 80 (2007) 166–174.